DOI 10.1007/s11182-022-02505-8
Russian Physics Journal, Vol. 64, No. 9, January, 2022 (Russian Original No. 9, September, 2021)

MODEL OF PLASTIC DEFORMATION AND FAILURE OF SOLIDS

L. B. Zuev, V. V. Gorbatenko, and L. V. Danilova

UDC 539.534.9

A model of localized plastic flow development based on the idea about interaction between plasticity carriers and acoustic emission pulses generated by developing elementary plasticity acts is proposed. It is shown experimentally that the plastic flow is always localized on the macroscopic scale level. The volume distribution of the localization zone has the form of different autowave processes and depends on the work hardening law.

Keywords: plasticity, deformation, defects, autowaves, failure.

INTRODUCTION

Experimental investigations of laws of plastic deformation in solids have shown that it is inhomogeneous at any stage. Universality of this statement has been checked on micro- [1], meso- [2], and macroscale levels [3], and it is possible to think that the multi-scale localization phenomena become essential practically simultaneously to the nature of plastic flow processes. In our research [3] it has experimentally been established that macrolocalization is obligatory for any materials and any loading conditions, and the forms of distribution of localization centers and the kinetics of their developments are correlated with the character of the plastic deformation curve of the material during the entire process of the plastic flow. In this case, the spatiotemporal localization structures arising in the sample spontaneously appear during plastic deformation with constant velocity and naturally evolve in time. As a result, the plastic medium during plastic flow is spontaneously stratified into volumes deformed and undeformed and spatially separated from each other at the examined time moments. Generally, such stratification of the deformable medium can be considered as its self-organization which Haken [4] understood as acquisition by the system of a certain spatial, temporal, or functional structure without specific influence from the outside. The feasibility of such treatment of the plastic flow localization has been proved by calculation [5] of the decrease in the system entropy during formation of localized plastic deformation regions which is a typical sign of the self-organization process [4].

The deformed and undeformed volumes of the material taken together form a *localized plasticity pattern* which reveals dynamic deformation macrostructures – *localized plastic flow autowaves* [3]. They were detected and studied by the method of speckle-photography modified for the analysis of plasticity [6] that allows step-by-step reconstruction to be performed of the displacement vector field $\boldsymbol{r}(x, y)$ of the deformable sample, its evolution to be calculated, and all components of the plastic distortion tensor

$$\beta_{i,j} = \nabla \boldsymbol{r}(x, y, t) \tag{1}$$

to be calculated as functions of the coordinates *x*, *y* and time *t*. Results of analysis of these experiments allowed us to conclude that evolving localized deformation patterns with characteristic inhomogeneity scale of $\sim 10^{-2}$ arose in samples during their plastic flow. The boundaries of localization layers can be fixed or can move with characteristic velocity

Institute of Strength Physics and Materials Science of the Siberian Branch of the Russian Academy of Sciences, Tomsk, Russia, e-mail: lbz@ispms.tsc.ru; gvv@ispms.tsc.ru; LidaAkvo@rambler.ru. Translated from Izvestiya Vysshikh Uchebnykh Zavedenii, Fizika, No. 9, pp. 75–83, September, 2021. Original article submitted February 15, 2021.

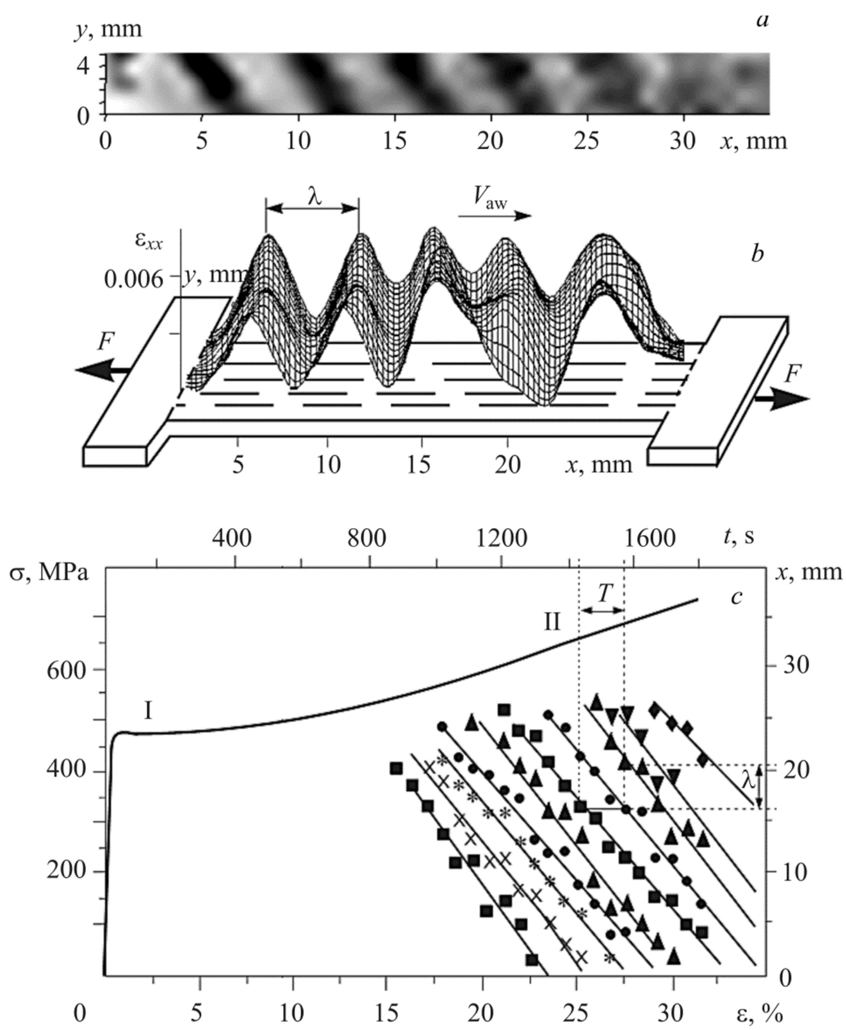

Fig. 1. Localization zones in the sample (dark bands) (*a*), spatial distribution of the ε_{xx} component of tensor (1) (*b*), diagram of the plastic flow σ(ε) and determination of the localized autowave plasticity parameters for a FCC Fe single crystal at the linear strain hardening stage (*c*).

$V_{\mathrm{aw}} \approx 10^{-5} - 10^{-4}$ m/s proportional to the velocity of the movable gripper of a test machine and typically exceeding it by an order of magnitude [7]. Examples of possible variants (patterns) of distribution of the localized deformation centers and explanation of the method of determining the spatiotemporal deformation process parameters are illustrated by Fig. 1.

In the present work, macroscopic laws of deformation localization pattern development at different stages of strain hardening are considered. The main problem is the construction of the model of plastic flow development based on an analysis of plastic flow localization pattern and its development upon tensile strain with a constant velocity.

WORK HARDENING AND LOCALIZED PLASTICITY PATTERN

As has already been established by the present time, the plastic flow localization is observed during plastic deformation of single and polycrystals of pure metals and alloys of different structures with FCC, BCC, HCP, and tetragonal lattices and nonmetallic materials (ceramics, alkali halide single crystals, and rocks). This gives us grounds to believe that it is the common feature of the plastic flow. On the other hand, it is also well known that the important characteristic of any plastic flow process is the presence of stages [1, 8]. Therefore, while studying the development of the localized plastic flow, it is pertinent to compare the localization pattern with the law of work hardening acting at the given stage of the deformation process. The latter can be characterized by the discretely changing hardening index *n* in the Ludwig equation approximating the stress-strain curve by the formula [8]

$$\sigma(\varepsilon) = \sigma_y + \theta\varepsilon^n . \tag{2}$$

Here σ and ε are the stress and strain, respectively; θ is the work hardening coefficient; and σ_y is the yield point. The stages of work hardening in the curve $\sigma(\varepsilon)$ are easily distinguished graphically as sections of the curve for which $n = \text{const}$. In particular, $n = 0$ on the yield plateau $(\sigma = \text{const};\ \theta = 0)$, $n = 1$ at the stage of linear work hardening $(\sigma \sim \varepsilon;\ \theta = \text{const})$, $n = 1/2$ at the stage of parabolic hardening, and $(\sigma \sim \varepsilon^{1/2})$ and $0 \le n < 1/2$ at the prefailure stage $(\sigma \sim \varepsilon^n)$.

A comparison of the plastic deformation stages with the localization pattern of the plastic flow showed that a certain variant of the pattern qualitatively independent on the particular details of the deformation mechanism and the structure of the deformable corresponds to each stage. This has allowed us to formulate the ***conformity Rule*** according to which motion of a solitary localized deformation center (the Lüders front) along the sample corresponds to the yield plateau, the motion with constant velocity of a group of equidistant localization centers corresponds to the stage of linear work hardening, the motion of the system of equidistant stationary deformation centers is characteristic for the parabolic stage of work hardening, and finally, mutually coordinated motion of the localized plasticity centers leading to their collapse is observed at the prefailure stage.

It was established that these laws are obeyed for all materials irrespective of their composition and structure as well as of the operating plastic flow mechanism (dislocation sliding, twinning, and deformation of phase transformation). Sufficiently wide variations of the structure and microstructure of the material cause only quantitative changes of localization patterns, remaining unchanged their main qualitative features. Thus, the plastic deformation is correlated in the entire volume of the sample, and the length $\lambda \approx 10^{-2}$ m mentioned above plays the role of the characteristic correlation radius of this process. The observed correlation forms are exhausted by the above-listed ones, and in all cases the number of forms coincides with the number of stages of the stress-strain curve observed in the material.

A comparison of the plastic flow localization pattern with the known descriptions of the general characteristics of autowave processes allowed us to establish that strictly defined observable autowave process mode can be put in correspondence with each stage of work hardening. Particularly, the yield plateau stage corresponds to the *switching autowave*, the linear work hardening stage corresponds to the *phase autowave*, the parabolic hardening stage corresponds to the *stationary dissipative structure,* and finally, the prefailure stage corresponds the *autowave collapse*. Thus, the plastic flow stages appear unambiguously related to the corresponding autowave types (modes). In other words, the plastic flow within the limits of the developed approach can be considered as natural evolution of autowave plasticity localization modes, developing from elastic deformation to failure in the strict sequence: *switching autowave → phase autowave → stationary dissipative structure → autowave collapse in the failure place*. The intermode transitions include creation of the chaotic quasi-homogeneous distribution of deformations over the volume having the scale $l < \lambda$ after failure of the structure, characteristic for the previous stage, and creation from chaos of a new autowave mode.

MODEL OF PLASTIC FLOW LOCALIZATION

The obtained experimental data suggest what exactly localization is the most important feature of deformation that determines its development. Based on the data about plastic flow localization, it is possible to formulate a number of fundamentally new representations about the nature of the plastic flow processes considered in this section. First of all, a close connection between pair products of the localized plasticity autowaves macroscopic parameters λ and V_{aw} and the characteristics of the crystal lattice of the materials: $\chi \approx 10^{-10}$ m – distances between densely packed planes and $V_t \approx 10^3$ m/s – the velocity of propagation of elastic transverse waves is found by means of analysis of the quantitative localization parameters at the stage of linear work hardening. In this case, the ratios of the velocities and scales had the same orders of magnitude $V_t/V_{aw} \approx \lambda/\chi \approx 10^7$–$10^8$. In the process of refinement of the ratios it was found that the equality

$$\left\langle \frac{\lambda V_{aw}}{\chi V_t} \right\rangle = \hat{Z} = 0.49 \pm 0.04 \approx \frac{1}{2} \tag{3}$$

holds true for the investigated materials, the validity of which is proved by a comparison of the ratios $\lambda V_{aw}/\chi V_t$ obtained for more than forty different materials [3, 9]. The angular brackets in Eq. (3) denote averaging over all these materials.

The products of χV_t with λV_{aw} having dimensionality of kinematic viscosity ($L^2 \cdot T^{-1}$) can be considered as characteristics of elastic and plastic deformation processes proceeding simultaneously in the deformable medium. They describe the redistribution of the elastic pressure with the velocity V_t and the characteristic scale of the order of χ and the redistribution of the localized plasticity regions with the velocity V_{aw} and the scale λ. Moreover, this law also shows the interrelation of the elastic $(\varepsilon_{el} << 1)$ and plastic deformations $(\varepsilon_{pl} \approx 1)$. The simplification used almost in any approach to the description of plastic deformation consists in the additive contributions of the elastic ε_{el} and plastic deformations ε_{pl}: $\varepsilon_{tot} = \varepsilon_{el} + \varepsilon_{pl}$. Because $\varepsilon_{el} << \varepsilon_{pl}$, the elastic contribution is usually neglected and $\varepsilon_{tot} \approx \varepsilon_{pl}$ is considered. However, equality (3) indicates incorrectness of such approach and suggests the expediency of the search for a closer interrelation between two deformation characteristics to create a new localized plastic flow model considering the close interrelation between the elastic and plastic deformation components in the course of plastic changing of the shape.

It seems reasonable to consider formula (3) which testifies to the important role of the acoustic subsystem of the crystal in the formation of autowave plasticity localization patterns as a basis for the model being developed. The deep sense of empirical equality (3) consists in the fact that it quantitatively relates the elastic wave characteristics $(V_t \text{ and } \chi)$ with the characteristics of the plastic flow localization autowaves $(V_{aw} \text{ and } \lambda)$. This fact has a simple explanation. According to Taylor–Orowan equation [1] $\dot{\varepsilon}_{pl} = b\rho_{mob}V_{disl}$, determining the plastic deformation rate $\dot{\varepsilon}_{pl}$ caused by dislocation motion, the direct contribution to the latter is given by mobile dislocations with the Burgers vector *b*, density ρ_{mob}, and nonzero motion velocity V_{disl}. The dislocation motion between local obstacles in the crystal is controlled by viscosities of phonon and electron gases [10] the states of which should be manifested through the plastic flow dynamics, including on the macroscale level.

Therefore, it is clear that the phonon subsystem plays an important role in the development of the localized plastic flow of solids. The matter is that the deformation process includes the interrelated events of two types coordinated in the deformable medium. On the one hand, these are jump-like relaxation events of motion dislocations, their ensembles, and in the macroscopic limit, deformation localization autowaves. On the other hand, each such event is accompanied by acoustic emission [11], that is, generation of elastic waves due to redistribution of elastic deformations during relaxation. The acoustic emission is widely used for nondestructive testing. In traditional approaches to plasticity studying, signals of acoustic emission are used to study the shear kinetics.

The acoustic pulse generated by an elementary shear, in turn, can initiate new shear due to the effect of acoustic plasticity that was also adequately studied in [12]. Thus, in the deformable medium co-exist and interact the phenomena of two types to which belong the dynamic subsystem of dislocation shears responsible for changes of the form, and the acoustic subsystem created by radiation of acoustic pulses, capable to excide new shears. This approach is in agreement with the idea that spontaneous stratification of the system into the interconnected information and dynamic subsystems [13] is necessary for self-organization. The interaction of such subsystems is justified by the following reasons. The appearance of new shears in the dynamic subsystem of moving dislocations and their ensembles is accompanied by emission of acoustic pulses (phonons). This leads to redistribution of the existing elastic field and, in its turn, initiates new relaxation shears accompanied by acoustic emission.

Thus, the development of the localized plastic flow in the model is controlled by acoustic emission pulses. An analysis of the well-known Wallner lines – notches on the surface of fragile spalls arising due to the curved growing crack fronts under the action of sound pulses emitted by the growing crack [14]. With that aim, we now estimate from below the energy necessary to bend the crack trajectory assuming that it is spent only to increase the fractured surface area ΔS. In accordance with experimental data [14], we obtain that $\Delta S \approx 10^{-8}$ m^2 for a surface notch depth of ~1 μm and a sample diameter of ~10^{-2} m. The pulse energy bending the crack front is $\Delta W \geq \gamma \Delta S \approx 10^{-8}$ J ≈ $6.25 \cdot 10^{11}$ eV for the surface energy density $\gamma \approx 1$ J·m^{-2} characteristic for metals. It is quite sufficient to activate new elementary plasticity acts.

It is possible to consider that equality (3) formalizes the relationship between the kinetic characteristics of subsystems – the velocity of elastic wave propagation (elasticity), on the one hand, and the velocity of dislocation motion in the regions subjected to the action of concentrators (plasticity at the expense of dislocation motion), on the other. In particular, the relationship between the acoustic and mechanical properties of a deformable solid is determined by the reverse action of the defect subsystem on the acoustic characteristics of crystals; as a result, the ultrasound velocity, for example, is a nonlinear function of the strain and flow stress $V_t(\varepsilon, \sigma)$ [15]. It remains constant at the stage of linear work hardening, decreases at the stage of parabolic hardening, and increases again when going to the prefailure stage.

The validity of the considered model is confirmed in principle by the analysis of spatial correspondence of the localized deformation centers and sources of acoustic emission signals. The experiments [16] with steel deformed by propagation of the Lüders front made it possible to establish that the observed localized plastic flow centers do serve as acoustic emission sources. In addition, it was revealed that the Lüders front moves inhomogeneously, and in places of its stop, centers of the corresponding stationary dissipative structure characteristic for the stage of parabolic work hardening are subsequently formed.

A comparison of the plastic flow localization patterns in solids with the data on their deformation mechanisms has allowed us to establish that the localization phenomena arise spontaneously at constant tensile velocity without special external action, and the localization patterns consistently change in the process of natural plastic flow development, and their evolution is closely related to the flow stages. In this case, the localization patterns at some stages possess clearly expressed spatial and temporal periodicity. Each of the localization patterns, as well as the phenomena at a corresponding stage of the flow process, is connected with specific microscopic mechanisms of work hardening acting at this stage, and the defect structure of the material and the characteristic of its work hardening change irreversibly during plastic flow, so that the deformable medium is essentially nonlinear [17].

Laws of macroscopic plastic flow localization are explained if the localization patterns are considered to be autowave processes in active media [17]. The autowaves are solutions of the differential parabolic equations $\dot{y} = \phi(x, y) + Dy''$, in particular, of the Kolmogorov–Petrovsky–Piskunov equations [18]. They are often used to describe self-organization of active media. The usual waves, for example, elastic ones, satisfy to the hyperbolic equations in partial derivatives $\ddot{y} = c^2 y''$. It is well known [17] that the description of autowave processes in active media required that the autocatalytic and inhibiting factors interconnected with each other must be taken into account. In a plastic flow, the strain ε is considered to be the catalyst, and the stress σ is considered to be the damper [3]. For this reason, the proposed model is called two-component (two-factor). The rates of change of the strain $\dot{\varepsilon}$ and the stress $\dot{\sigma}$ in this model are determined by the parabolic equations of the form

$$
\begin{cases}
\dot{\varepsilon} = f(\varepsilon, \sigma) + D_{\varepsilon}\varepsilon'', & (4) \\
\dot{\sigma} = g(\varepsilon, \sigma) + D_{\sigma}\sigma'', & (5)
\end{cases}
$$

where the nonlinear *N*-shaped functions $f(\varepsilon, \sigma)$ and $g(\varepsilon, \sigma)$ are the local kinetic changes of strain and stress, respectively, and terms with the second spatial derivatives describe the redistribution of the strain and stress. It is possible to accept that owing to Eq. (3), $D_{\varepsilon} \approx \lambda V_{aw}$ and $D_{\sigma} \approx \chi V_t$. The analysis [3] of possible solutions of system (4) and (5) has shown that they generate different types of autowave processes depending on the work hardening law acting at the corresponding stage of the plastic flow process.

Let us consider some characteristic details of the evolution of the flow localization pattern at the successive deformation stages in connection with changes of the defect structure of the material during the process. In particular, it is well known that the single Lüders front characteristic for the yield plateau stage divides the elastically and plastically deformed volumes of the material, and during its propagation, the volume of the first decreases, and of the second increases. This means that the irreversible transition of the deformable medium to the new state with larger number of defects and capability to be deformed plastically by dislocation slip takes place at the Lüders front; moreover, subsequent unloading of the medium does not restore its initial properties. At the stages of linear and parabolic work hardening, the defect structure in local volumes of the sample changes periodically, and these changes are directly related to the macroscopic plastic flow inhomogeneity (localization).

Within the limits of such analysis, the localized deformation centers can be interacted through the exchange phonon interaction. In this case, it is expedient to put in correspondence to the autowave a localized deformation quasiparticle – *autolocalizon* [19] the mass of which is completely determined by the autowave parameters. Such step corresponds to the concept of quasiparticles in the theory of solids [20]. One of the first attempts of introduction in strength and plasticity physics of the quasiparticle corresponding to the crack distribution – *crackon* – has been undertaken by Morozov *et al.* [21] to analyze fracture. The introduction of the autolocalizon leads to important consequences. Thus, using the de Broglie formula, we rewrite equality (3) in the form

$$
\frac{h}{\lambda V_{\mathrm{aw}}} \approx 2\frac{h}{\chi V_t}, \tag{6}
$$

where *h* is Planck's constant. Obviously, it is equivalent to the equality $m_{a-l} \approx 2m_{\mathrm{ph}}$, where $m_{a-l} = h/\lambda V_{\mathrm{aw}}$ is the autolocalizon mass, $m_{\mathrm{ph}} = h/\chi V_t$ is the phonon mass, and Eq. (6) corresponds to the mechanism of dislocation creation in crystals due to phonon condensation proposed by Umedzawa *et al.* [22].

At the prefailure stage when the work hardening index in Eq. (2) is $n < 1/2$, physically very interesting situation is observed. The collapse of the localized deformation autowave at this stage terminates the plastic flow process, the localized plasticity autowave collapses in the place of future failure of the sample, and the macroscopic deformation localization becomes such that the volume of plastically deformable material decreases and finally, a neck arises preceding the formation of a viscous crack. At this stage, a section can be observed on the deformation diagram shown in the conditional stress-strain coordinates for which the work hardening factor is negative.

Examples such localized plasticity autowave collapses for aluminum and titanium are shown in Fig. 2. It can be seen that from the beginning of the prefailure stage with $n < 1/2$, the centers fixed at the stage of parabolic hardening start to move along the sample axis approaching to high-amplitude stationary zones. The special feature of such motion is the consistency of center motion, because of which all of them reach the fixed localization zone almost simultaneously. In this case, the plots of time dependences of mobile center position $X(t)$ form bundles of straight lines with coordinates of the centers X^* and t^*. The straight lines in the bundles approaching to the fixed zone from different sides have slopes of different signs, and those approaching to the fixed zone from one side have slopes with one sign. During deformation process, some localized deformation centers moving at this stage can appear or disappear stopping their development.

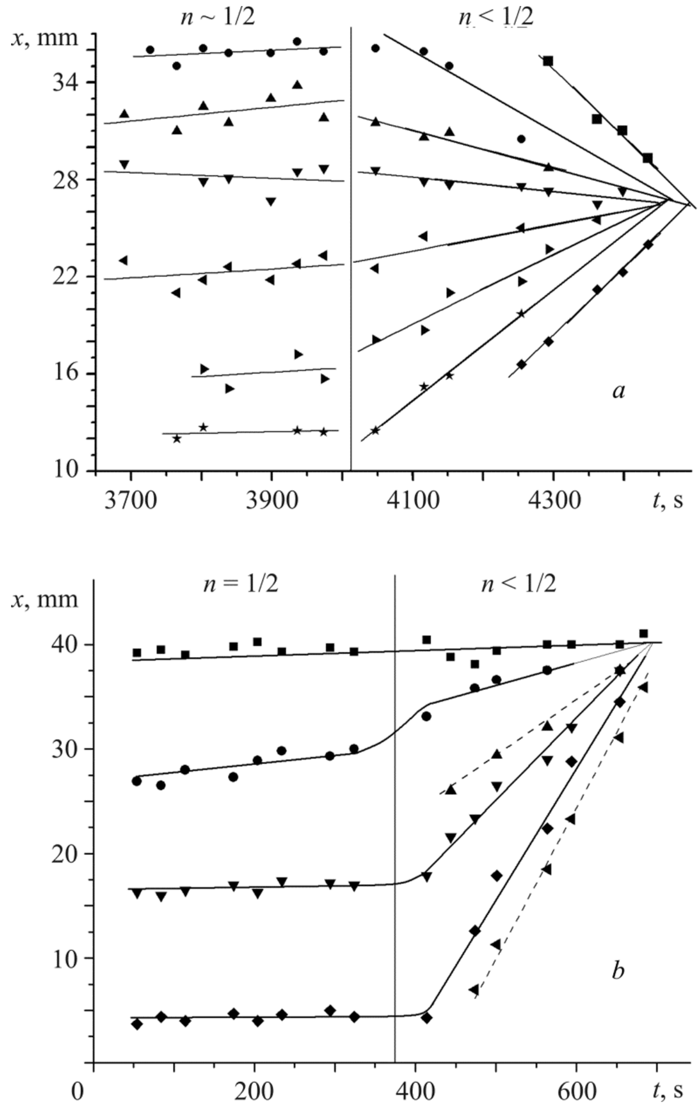

Fig. 2. Diagrams of the localized plastic flow in aluminum (*a*) and titanium (*b*).

To describe the kinetics of the centers at the prefailure stage at the stage of the localized plasticity autowave collapse, it is convenient to affix the origin of coordinates to a certain fixed localization zone. In this case, the coordinate of the *i*th center ξ_i determines its velocity

$$V_i(\xi) = \alpha\xi_i + \alpha_0 , \qquad (7)$$

where α and α_0 are empirical constants different for different materials. To understand the meaning of Eq. (7), we now consider that at the beginning of the prefailure stage, the macrolocalization center is symmetrically surrounded by neighboring centers since $\lambda = \mathrm{const}$ at the stage of parabolic hardening. In this case, a decrease in the distance between the centers with identical deformation fields creates the repulsive force explaining why the centers created at large distances from the place of future failure move with higher velocities, according to Eq. (7). Assume that the velocity of the localized plasticity centers is the thermally activated process described by the standard relation

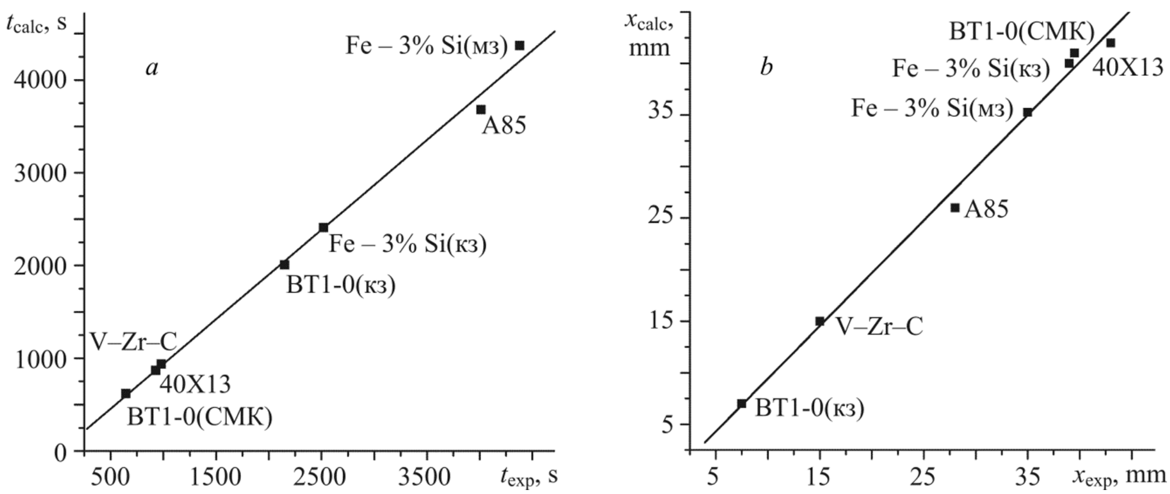

Fig. 3. Correlation settlement and experimental data about failure of alloys: *and* – for the failure moment, – for a failure place. Factors of correlation of compared sizes ~0.95.

$$V_{\text{aw}} = V_0 \exp\left(-\frac{U - \gamma\sigma}{k_{\text{B}}T}\right) = \Omega \exp\left(\frac{\gamma\sigma}{k_{\text{B}}T}\right), \tag{8}$$

where the multiplier $\Omega = V_0 \exp(-U/k_{\text{B}}T)$ for the examined material depends only on temperature T, γ is the activation volume, U is the activation, k_{B} is the Boltzmann constant, and V_0 is a constant. The stress initiating the center motion can be written as $\sigma \approx \sigma_f - \sigma_{\text{obs}}$, where σ_f is the flow stress in the sample, and the contribution from the fixed obstacle σ_{obs} decreases with increasing distance to it, that is, $\sigma_{\text{obs}} \sim 1/\xi$. A fixed high-amplitude localized plasticity center created in the end of the parabolic stage and defining the place of future failure (neck) can be considered as such obstacle. Taking into account an increase in the number of the centers and the stress decay with distance, we can write $-d\sigma_{\text{obs}}/d\xi \sim 1/\xi$, from which it follows that $\sigma_{\text{obs}} \sim \text{const} - \ln\xi$. The substitution of the last formula in Eq. (8) leads to the proportionality relation $V_{\text{aw}} \sim \xi$, that is, to Eq. (7).

Experimental data for different materials showed that X^* and t^* values practically coincide with the experimentally determined coordinate and time of sample failure in natural tests. This suggests that they correspond to the place and time of crackon creation. Obviously, the X^* and t^* values can be determined by extrapolation of the dependences $X(t)$ at large times. After that, the problem on the possibility of determining positions of motion diagram centers at the prefailure stage becomes important. These data can be used to predict the time and place of the future failure. The pole position and hence, the time and place of failure can be predicted already upon strains of 0.3−0.65 of the strain before failure of samples of investigated materials. A comparison of the calculated and actual coordinate and time of the failure shown in Fig. 3 demonstrates that these values are linearly correlated, and the spatiotemporal coordinates of the pole of diagrams of center motion at the prefailure stage almost coincide with the place and time of the actual failure.

Critical values of parameters also X^* can t^* be defined from dependences (7) from the relations $X^* = \alpha_0/\alpha$ and $t^* = t_0 + 1/\alpha$, where t_0 is the time of beginning of the collapse stage. Figure 3 shows the data on the correlation of the calculated and experimental values. These data demonstrate the possibility of prediction of the place and time of failure of objects before the manifestation of external signs of failure upon general deformation, sufficiently distant from the maximal elongation of the sample at rupture. For this purpose, it is sufficient to extrapolate the dependences

$X(t)$ to their crossing in the center. This procedure is promising for the development of a new method of prediction of viscous failure, for example, for metal processing under pressure. Thus, Zavodchikov *et al*. [23], using these procedures, succeeded in revealing the reason for rupture of Zr− 1 wt% Nb alloy billet subject to cold rolling of thin-wall pipes for heat releasing elements of nuclear power reactors. The analysis of the autowave patterns has allowed regions of residual stress jumps to be detected along the boundaries of which billets failed during cold rolling.

CONCLUSIONS

In this work it has been shown that the plastic flow in solids is macroscopically localized along the entire plastic flow curve from the yield point the strength limit. During the process, the limited number of localization forms is implemented, each of which depends on the acting law of work hardening and is closely related with it. For this reason, when analyzing the plastic flow during the entire process, it should be taken into account that irrespective of the special features of the process and even its micromechanism, the autowave laws do exist common for all solids.

According to them, the plastic flow kinetics is determined by laws of changing the forms of macroscopic deformation localization, that is, successive generation of several localized plastic flow autowave modes and formation of work hardening localization pattern unambiguously corresponding to the stage. Based on this, is possible to assume with confidence that the autowave localization patterns can be used to predict and to explain the special features in the behavior of materials under loading.

This work was supported in part by the State Assignment to the Institute of Strength Physics and Materials Science of the Siberian Branch of the Russian Academy of Science (Theme Number FWRW-2021-0011).

REFERENCES

1. D. Hull and D. J. Bacon, Introduction in Dislocations, Elsevier, Oxford (2011).
2. V. E. Egorushkin and V. E. Panin , Fiz. Mezomekh., **20**, No. 1, 5−13 (2017).
3. L. B. Zuev, Autowave Plasticity. Localization and Collective Modes [in Russian], Fizmatlit, Moscow (2018).
4. G. Haken, Information and self-organization. A Macroscopic Approach to Complex Systems, URSS, Moscow (2014).
5. L. B. Zuev, Phys. Wave Phenom., **20**, No. 3, 166–173 (2012).
6. A. B. Kudrin and V. G. Bakhtin, Applied Holography. Research of Processes of Metal Deformation [in Russian], Metallurgiya, Moscow (1988).
7. L. B. Zuev, S. V. Kolosov, and M. V. Nadezhkin, Russ. Phys. J., **63**, No. 5, (2020).
8. J. Pelleg, Mechanical Properties of Materials, Springer, Dordrecht (2013).
9. L. B. Zuev, S. A. Barannikova, V. I. Danilov, and V. V. Gorbatenko, Prog. Phys. Met., **22**, No. 1, 3−57 (2021).
10. D. N. Blaschke, E. Motolla, and D. L. Preston, Phil. Mag., **100**, No. 5, 571−600 (2020).
11. V. S. Boiko, R. I. Garber, A. M. Kosevich, Reversible Plasticity of Crystals [in Russian],Nauka, Moscow (1991).
12. G. A. Malygin, Fiz. Tverd. Tela, **42**, No. 1, 69−75 (2000).
13. V. V. Kadomtsev, Usp. Fiz. Nuk, **164**, No. 5, 449−530 (1994).
14. B. A. Drozdovskii and Ya. B. Friedman, Influence of Cracks on Mechanical Properties of Structural Steels [in Russian], Metallurgiya, Moscow (1960).
15. L. B. Zuev and B. S. Semukhin, Phil. Mag. A, **82**, No. 5, 1183−1190 (2002).
16. E. S. Nikitin, B. S. Semukhin, and L. B. Zuev, Pis'ma Zh. Tekh. Fiz., **34**, No. 15, 70−74 (2008).
17. M. A. Lebyodkin, D. F. Zhemchuzhnikova, T. A. Lebedkina, and E. C. Aifantis, Res. Phys., **12**, No. 5, 867−869 (2019).
18. V. A. Vasilev, Yu. M. Romanovskii, and V. G. Yakhno, Autowave Processes [in Russian], Nauka, Moscow (1987).
19. L. B. Zuev and S. A. Barannikova, Metals, **10**, 1−15 (2020).

20. N. B. Brandt and V. A. Kul'bachinskii, Quasiparticles in Condensed State Physics [in Russian], Fizmatlit, Moscow (2007).
21. E. M. Morozov, L. S. Polak, and Ya. B. Friedman, Dokl. Akad. Nauk SSSR, **146**, No. 3, 537–540 (1964).
22. H. Umedzawa, H. Matsumoto, and M. Tachiki, Thermo Field Dynamics and Condensed States, [Russian translation], Mir, Moscow (1985).
23. S. Yu. Zavodchikov, L. B. Zuev, and V. A. Kotrekhov, Metal Science Issues of manufacturing Zirconium Alloy Products [in Russian], Nauka, Novosibirsk (2012).